Egypt. J. Soil Sci. **Vol. 62,** No. 3, pp. 223 - 23 (2022)

Egyptian Journal of Soil Science

http://ejss.journals.ekb.eg/

Performance of Fast and Slow Phosphorus Release from Nano-Bone Char

Ahmed A. El Refaey[1*], Naglaa A. Mohamed[1], Hamida E. Mostafa[2], Neama A. Gouda[3]

[1] *Soil& Water Science Department, Faculty of Desert and Environmental Agriculture, Fuka, Matrouh University, Egypt*
[2] *Soil& Water Science Department, Faculty of Agriculture, El-Shatby, Alexandria University, Egypt.*
[3] *Chemistry of Pesticides Department, Faculty of Desert and Environmental Agriculture, Fuka, Matrouh University, Egypt*

Abstract

The study investigates the release of phosphorus (P) from nano-bone char (Nano-BC), which could be a potential P-soil fertilizer. The study evaluated the performance of P releasing from Nano-BC compared to the originated bone char (BC) which was prepared under pyrolysis temperature 650^{o}C.BC and Nano-BC were characterized by elemental composition, X-ray diffraction (XRD), surface areas, Fourier transform infrared (FTIR), and scanning electron microscopy (SEM), showing the physicochemical properties differences.The P-fast release was determined after 24 hours under different conditions (pH, ionic strength, and coexisting ofanion species), while the P-slow release was after 21 days. The performance of P-fast release from Nano-BC was higher than from BC, acidic conditions were more suitable with the privilege for Nano-BC. Higher ionic strength gave the lowest P-releasing amounts for both materials (0.47 to 0.51 mg.g^{-1} for BC and 0.61 to 0.62 mg.g^{-1}for Nano-BC). The coexisting $SO_4^{=}$anion encouraged the rapid release of P from Nano- BC (8.65 mg.g^{-1}) than those for Cl^- and NO_3 anions. For the slow release experiments, Nano-BC gave higher P- release than BC withpH ranging from 4.25 to 9.39 for Nano-BC and 4.75 to 9.75 for BC. The pseudo-second-order kinetic model was correlated quite to the release of ortho-P (R^2 = 0.894, and 0.901for BC, Nano-BC, respectively) and this indicated the chemical nature of the release process of ortho- P. The results could suggest the privilege of using Nano-BC as a soil P fertilizer.

Keywords: Nano-bone char; Phosphorous release; Kinetics

Introduction

Phosphorus (P) is an essential macronutrient that is critically needed for the normal functioning of ecosystems and has no substitute in food production. Agriculture soils face several challenges due to fast increases in food demand and limited resources. The availability of soil native P to plant growth and organisms' propagation is seldom covering their requirements and thus application of P fertilizers is recommended to increase soil productivity. According to the P fertilizer industry records, phosphate rock is a non-renewable raw material of P, which is going towards depletion (Koppelaar and Weikard, 2013). It is estimated that demand would outstrip the supply of rock phosphate within the next century (Smil, 2000; Cordell et al., 2009; Gilbert, 2009). Phosphorus scarcity challenge means that other sources of P have to be recovered for reuse as fertilizers to substitute phosphate rock (Cordell et al., 2011). Phosphorus recovery from waste materials is considered one of the major solutions to overcome the current depletion of mined-P resources all over the world. Economically and technically, the recovery of P from animal wastes is the most suitable and tractable solution (Rittmann et al., 2011).

Recently, several studies have pointed out the role of bone char in water/wastewater treatment applications for removing organic such as surfactants and industrial wastes (Hashemi et al., 2013; Mesquita et al., 2018), inorganic pollutants such as fluoride (Medellin-Castillo et al.,2014; Brunson et al., 2014) and heavy metals (Cu,Cd, Ni, and Zn) (Wilson et al., 2003; Ko et al., 2004; Leyva-Ramos et al., 2010; Rocha et al., 2011; Hernández-Hernández et al., 2017)

*Corresponding author e-mail: ahmedelrefaey@alexu.edu.eg
Received: 20/7/2022; Accepted: 25/8/2022
DOI: 10.21608/EJSS.2022.151212.1519

as well as an economic and alternative phosphorus fertilizer (Warren et al. 2009; Weber et al., 2014; El-Refaey et al., 2015; Zwetsloot et al., 2014 and 2016; Buss et al., 2016; Mahmoud et al., 2017). Bone char is composed of a mix of carbon and calcium phosphate (Bioapatite). Bioapatite is similar to hydroxyapatite, with more complex imperfect containing relatively abundant other cations like Mg, and Na (Elliott, 2002; Cazalbou et al., 2004; Pasteris et al., 2012).The apatite content, precariously crystallized in bone char could be effective as mineral P fertilizers besides low concentrations of heavy metal contents and isa more economical alternative (Deydier et al., 2005; SiebersandLeinweber, 2013; Weber et al., 2014; El-Refaey et al.,2015; Zwetsloot et al., 2014 and 2016; Buss et al., 2016; Mahmoud et al., 2017). Nanotechnology has been tremendous growth in the present decade, and it has improved and impacted a measurable effect on all the sectors in society, such as medical, food, engineering, polymer sector, electronics, etc. Nevertheless, in the agricultural sector, the agricultural diagnostic, the remediation of soil and water pollution monitoring, sustainable agriculture, nano pesticides, precision farming section, and fertilizers could be improved, but nanotechnology in the applications of the agricultural sector is still relatively under development, especially in the fertilization (DeRosa, 2010; Mastronardi et al., 2015; Mahmoud et al., 2020; Mahaletchumi, 2021; Ibrahim and Hegab; 2022).

Therefore, the main objective of this study is to evaluate the P- released from Nano-BC as a P- source compared to BC. The influence of different conditions (pH, ionic strength, and coexisting anions) on the fast P release (during 24 h) was studied. In addition, the slow P-releasing experiment (21 days) was conducted to study the behavior of orthophosphate release from Nano-BC to BC**.**

Material and Methods

Materials Preparation

The used bones in these experiments were collected from the local market in Alexandria, Egypt. Primary bones were cleaned several times with distilled water, then dried at 105 °C for 48 h, and screened and cut less than 5 cm for preparing bone char. To prepare bone char, prepared bone was pyrolyzed for 2 h at 650 °C with a heating rate increase of 25 °C.min^{-1} in a muffle furnace according to El-Refaey et al. (2015). The obtained BC was ground and sieved through 0.5-mm plastic screen and part of the 0.5mm BC was ground for nano-scale by mechanical ball mill RWTCH Planetary Ball mill type (RM400).

Materials characterization

BC and Nano-BC were characterized by chemical compositions, surface areas, X-ray diffraction (XRD), Fourier transform infrared (FTIR), and scanning electron microscopy (SEM). For phosphorus and elemental contents of BC and Nano-BC, 2 g of the sample was added to 25 ml of Aqua regia (3:1 of Hydraulic acid (12N) to Nitric acid (15N)) in a 125-mL flask, the solution was heated on a hot plate and boiled until complete evaporation, without burning the residue. After cooling, 2.5 ml of Nitric acid (2 N) was added to the residue and the clear solution was transferred to 25-mL volumetric flasks and completed the volume with distilled water. Phosphorus was determined by the vanadomolybdic acid method (Chapmann and Pratt, 1961), complexiметric EDTA titration was employed for determining calcium and magnesium simultaneously and individually (Lanyon et al., 1982), and organic carbon contents were determined combustion method (Black et al.,1965).

X-ray diffraction (XRD) was conducted for Nano-BC and BC by X-ray Powder Diffraction -XRD-D2 PhaserBruker (Germany) using the Cu Kα radiation ((λ=1.541 Å) at 30 kV and 10 mA. The diffractogram was scanned from (2θ) 5 to 60 ◦.

BET-surface area was obtained from analysis of nitrogen adsorption isotherms at 77 ˚K using Beckman Coulter SA(TM) 3100 Surface Area and Pore Size Analyzer, Beckman Coulter, Nyon, Switzerland. Pore volume was determined by Barret–Joyner–Halender method from the N_2desorption isotherms (Nader, 2015; El Refaey, 2021).

In order to identify the functional group composition, Fourier transform-infrared (FTIR) spectra at the range 400 – 4,000 cm^{-1} by KBr pellet technique was conducted using Bruker Tensor (37) FTIR spectrometer.

The surface morphology of BC and Nano-BC were examined by Scanning electron microscopy (SEM) using a Jeol JSM-5300 scanning electron microscope and was operated at 15 - 20 kV. Samples were gold-coated in a sputter coating unit (JFC-1100 E) before SEM examines. Transmission electron microscopy (TEM) for the Nano-BC sample was conducted using Jeol, TEM-1400Plus electron Microscope.

Phosphorus release experiments

Fast P release experiment

For fast P release experiments, 0.2 g each of Nano-BC, and BC (0.5 mm) were incubated into a plastic tube containing 50 mL of distilled water for 24 h at 30 rpm and 27°(room temperature). The initial pH was adapted to 3, 5, 7, 9, and 11 by 1.0 mM HCl or NaOH. Then, samples were centrifuged and filtered through a 0.45-µm filter for P measurements. The ionic strength effect on P release was conducted by the same proceeds under various KCl levels (0, 0.05, 0.1, and 0.2 mol·L^{-1}). For examiningthe effect of anion species in the solutions, three materials were tested under 0.1 mol·L^{-1}KCl, KNO_3, and K_2SO_4, respectively**.**

Slow P release experiment

0.5g of BC or Nano-BC sample into 500 mL of distilled water was added into each Erlenmeyer flask without pH adjustment. The flasks were then stirred at room temperature for 21 days. The samples were withdrawn almost every time interval (2 days). The withdrawn samples were filtered and the ortho-P concentrations in the supernatant were determined and the pH was recorded. The orthophosphate concentration for fast and slow experiments was determined by the molybdate-ascorbic acid method (Olsen and Sommers, 1982) at wavelength 882 nm.The P release amount from tested sources q (mg.g^{-1}) was estimated from the following equation:

$$q=(Ci\ V)/m \qquad (1)$$

Where C_i(mg/L) is the equilibrium P concentration at every interval time; V (L) is the water volume and m (g) is the added P-source materials amount.

Results and Discussion

Materials characterization

Some characteristics,including phosphorus, calcium, and carbon content composition and surface area and total pore volume,are shown in Table (1).The contents of phosphorus and calcium in nano-bone char (Nano-BC) were greater than the originated bone char (BC). So the ratio of Ca:P increased by converting BC to Nano-BC. Otherwise, organic carbon contents decreased as a result of converting BC to nano-BC from 4.84% to 2.05, respectively. Also, results indicated the increase of BET-surface area and total pore volume as results of turning the BC to nano scale (Kalia and Kaur, 2019; El-Ramady et al., 2021).).

TABLE 1. Some characteristics of bone char (BC) compared to nano-bone char (Nano-BC)

	%				Surface area $m^2\ g^{-1}$	Total pore volume $cm^3\ g^{-1}$
	P	**Ca**	**Mg**	**C**		
BC	7.72	0..94	0.64	4.84	94.66	0.317
Nano-BC	9.56	1.08	0.67	2.05	108.32	0.347

X-ray diffraction (XRD)

As shown in Fig. (1), the X-ray diffraction (XRD) for both bone char (BC) and nano-bone char (Nano-BC) presented an approximate similar degree of lattice between the structures (2Θ). Bone char mainly consists of calcium phosphate, calcium carbonate and carbon (El-Refaey et al. 2015; Younesi et al., 2011; Flores-Cano et al., 2016; Maeda et al., 2019). Also, XRD patterns confirmed an increase in the intensity of the nano-bone char peaks than the original bone char with peaks shifting corresponding to the crystal structure. A lower degree of crystallization of BC was shown than in nano-BC structure. This could be explained by the decrease of organic carbon associated with the structural composition of Nano-BC. Rojas-Mayorga et al. (2013) reported an increase in the Ca/P ratio correlates with a crystallinity index, especially with a decreased in the presence of carbonates.

Fourier-transform infrared spectroscopy (FTIR)

The BC and Nano-BC FTIR spectra are shown in Figure (2). Generally, bone char spectra had the following peaks 3426, 2200.06, 2012.76, 1633.85, 1461.07, 1415.36, 1033.36, 872.38, 604.45, 566.79, and 470.64 cm^{-1}, correspond to the BC structure which includes carbonate groups, phosphate groups, and organic phase. The band located at 3426.77 cm^{-1} is attributed to O–H (hydroxyl) (Rojas-MayorgaetaL., 2013; Manalu et al., 2015; Azzaouia et al., 2017; Saleh et al., 2020). The peak at 2200.06 cm^{-1} and1633.85 cm^{-1} are attributed to the bone organic phase vibration, Alkyne C≡C and C=C aromatic, respectively (Rojas-Mayorga et al., 2013; Saleh et al., 2016; Hernández-Hernández et al., 2017).

The stretching peaks at 2012.76, 1033.58,604.45 and 566.79 cm^{-1} can be attributed to PO_4^{3-}stretching vibrations (França et al., 2014; Azzoui et al., 2015; Manalu et al., 2015; Hernández-Hernández et al., 2017; Saleh et al., 2020) The peaks at 1461.08, 1415.36 and 872.38 cm^{-1}can be assigned to CO_3^{2-} (Rojas-Mayorga et al., 2013; Manalu et al., 2015; Hernández-Hernández et al., 2017). Similar bands appeared with nano-BC spectra with little modification or shifts of bands with the emergence of somenew peaks.

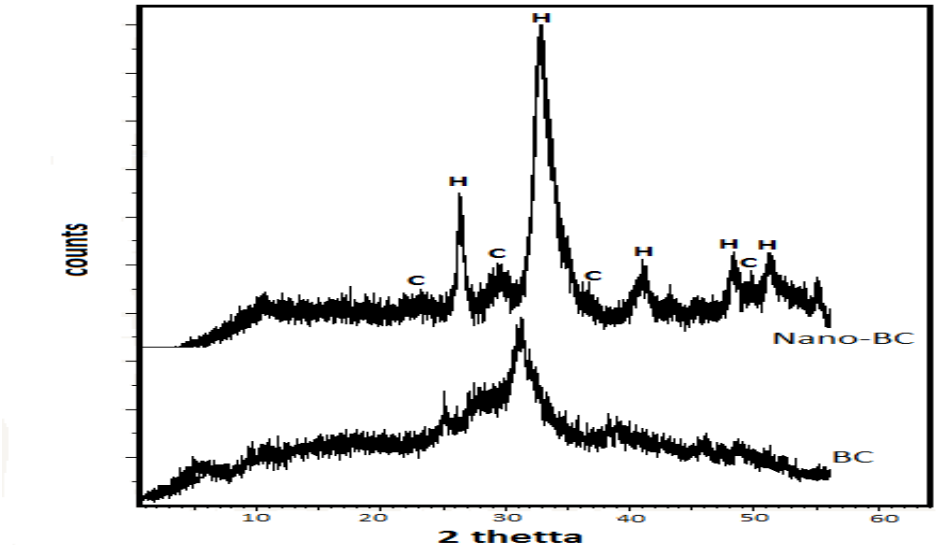

Fig. 1. XRD patterns of bone char (BC) and nano-bone char (Nano-BC)
(C: Calcite; H: hydroxyapatite)

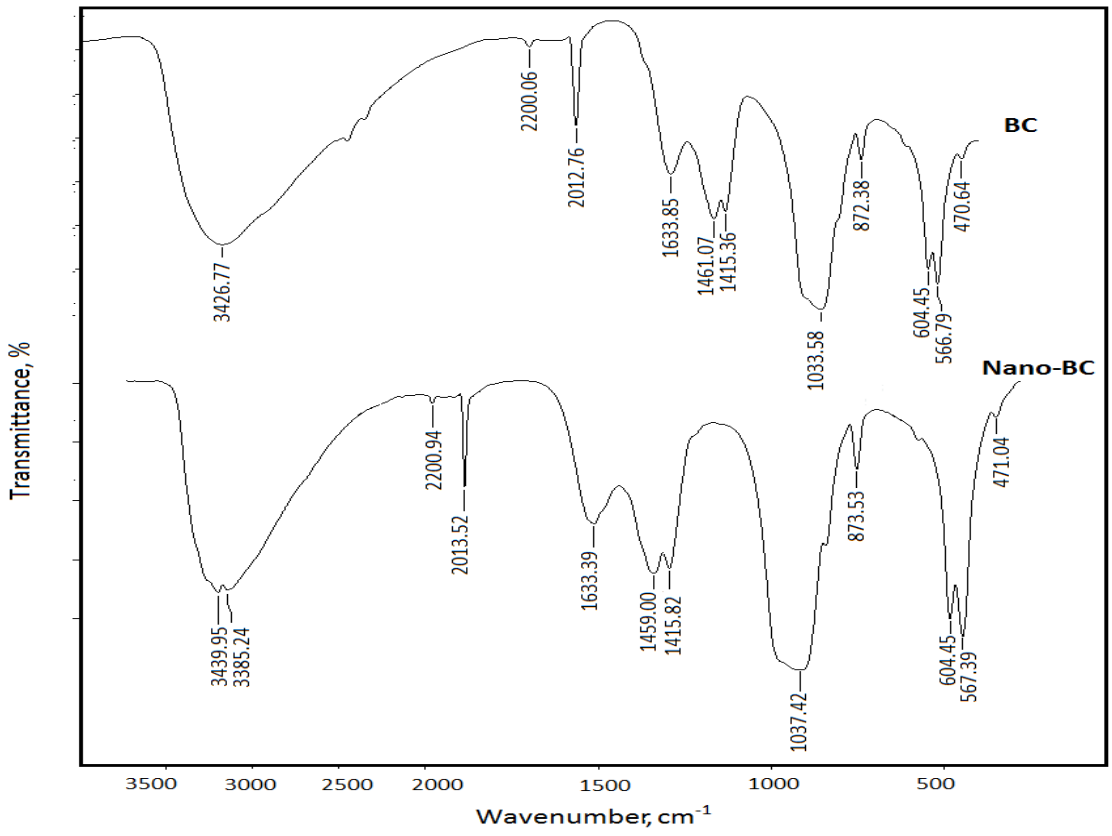

Fig. 2. FTIR spectra of bone char (BC) and nano-bone char (Nano-BC)

Morphological characterization

The results of SEM and TEM could indicate and help in data explanations. The morphological analyses are shown in Fig. (3). BC revealed porous and agglomerated structures as a result of pyrolysis temperature (Patel et al. 2015; Saleh et al., 2020). The SEM image of the nano-BC represented the nano-particles are mostly spherical with some re-aggregated particles and the typical single-particle sizes are in the range of 45 to about 49 nm as indicated by the TEM image (Fig.3).

Fast release of P

Influence of pH

The effect of different pH (3, 5, 7, 9, and 11) on P release from bone char (BC), and nano-bone char (Nano-BC), and is shown in Fig.(4-A). The results demonstrated that the fast ortho-P release after 24 decreased with increasing the pH with noticeable privileges to bone char (BC), than nano-bone char (Nano-BC). This could be explained as the P release process as pH-dependent. And, the restraining of the P-release species of the bone char materials could give them sustainable P release performance under different soil conditions. In addition, Nano-BC at a low pH value of 3 the P- released gives the highest value (26.21 mgP g^{-1}). The high ortho-P release at low pH could be simply clarified by the metallic phosphate species dissolution at acidic circumstances. For bone char, some P- species (such as pyrophosphate) may be bonded to charred materials (BC and Nano-BC) surface, by H-bonding, so that could be pH sensitive and liable to water dissociation (Chen et al., 2015).

Influence of ionic strength and coexisting anion

The effect of different ionic strengths on ortho-P release from bone char (BC), and Nano-bone char (Nano-BC) is shown in Fig (4-B). As observed, the discharge of ortho-p decreased with increasing the KCl concentration for BC and Nano-BC and there were no significant differences between Nano-BC and BC and released about 0.47 to 0.51 mg.$g^{-1}$for BC and 0.61 to 0.62 mg.$g^{-1}$for Nano-BC. The completion between Cl^- ions and adsorptive site for PO_4^{3-} and HPO_4^{2-}, could be difficult for BC and Nan-BC for their complex structure.

The effects of different coexisting anions (Cl^-, NO^-_3, and SO^{2-}_4; as 0.1 M solution of KCl, KNO_3, and K_2SO_4, respectively) on P release from BC, and Nano-BC were represented in Figure (4-C). As shown in Fig. (4-C), for BC and Nano-BC, there was no significant difference between Cl^-, and NO^-_3 coexisting anions compared to blank water. The high ortho-P released was achieved by $SO_4^{2-}$with Nano-BC (8.65mgP g^{-1}). That could be due to the occupation of SO_4^{2-} more active sites onNano-BC than Cl^- and NO_3^-(Chouyyok et al., 2010; Qian et al, 2013; Liu et al., 2021) and also, the competition between sulfate and PO_4^{3-} and HPO_4^{2-} for bonding with Ca^{2+} and Mg^{2+} could enhance the released P (Chouyyok et al. 2010; Liu et al., 2021).

Slow release of P

The orthophosphate (ortho-P) form is the most easily uptake than the other forms (Buss et al., 2020). The release of orthophosphate from bone char (BC), and nano-bone char (Nano-BC) was determined in the slow P release experiments during the 21-day release cycle (Fig.5-A).The changes in pH in the solution during the slow release experiment were presented in Fig. (5-B). It can be seen that the released P increased from BC and Nano-BC with time with privileges for Nano-BC to reach 0.453 mg.g^{-1} after 20 days. This increase in P-released value is accomplished by increasing the pH of the solution. The pH values of Nano-BC were lower than BC at the first week of the experiment, and gradually began to increase with time from 4.25 to 9.39 for Nano-BC and from 4.75 to 9.75 for BC during the 21 days.

Kinetic release studies

The P release was fitted with fractional power, Elovich, pseudo-first-order, pseudo-second-order, and intra-particle diffusion kinetic models, linear forms are reported in Table (2) (El-Refeay, 2021).

TABLE 2. The linear form of the used kinetics models

Model	linear form equation
fractional power:	$\ln q_t = \ln a + b \ln t$
Elovich:	$q_t = \frac{1}{\beta}\ln(\alpha\beta) + \frac{1}{\beta}\ln t$
pseudo-first-order:	$\log(q_e - q_t) = \log q_e - k_1 t/2.303$
pseudo-second-order:	$\frac{t}{q_t} = {}^{1}/_{k_2 q_e^2} + {}^{t}/_{q_e}$
intra-particle diffusion:	$q_t = k_i t^{1/2} + C$

Where: q_e (mg/L) and q_t(mg/L) represent the P concentration in the solution at equilibrium and at a time t; a and b are constants with b < 1; α equals primary coefficient (mg.$g^{-1}$$day^{-1}$); β equals desorption coefficient (g mg^{-1}); k_1 equals the pseudo-first rate constant (day^{-1}) and $k_2$equals the pseudo-second-order model rate constant (g· mg^{-1} day^{-1}), respectively; k_i (g mg^{-1} $day^{-1/2}$) represent the intra-particle diffusion rate constant; C is constant (mg g^{-1}) related to the boundary layer thickness.

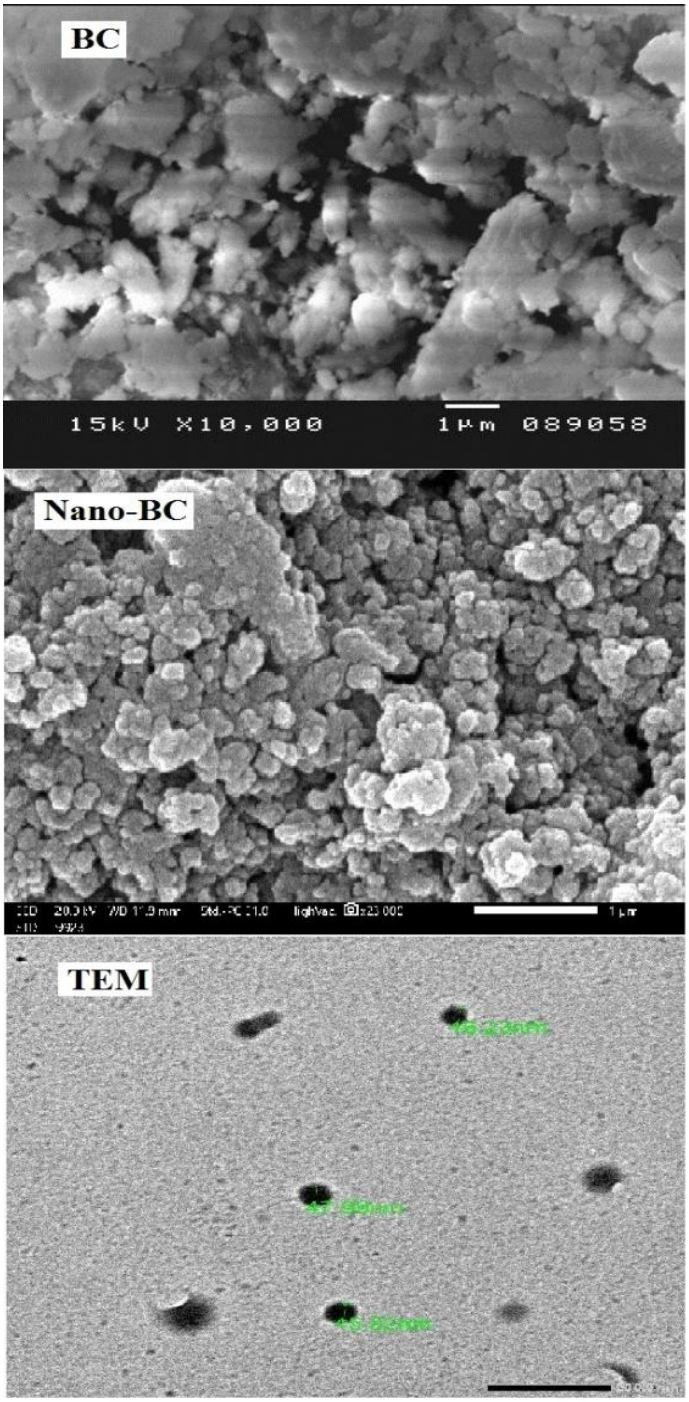

Fig. 3. SEM for bone char (BC), and nano-bone char (Nano-BC), and TEM micrographs for Nano-BC

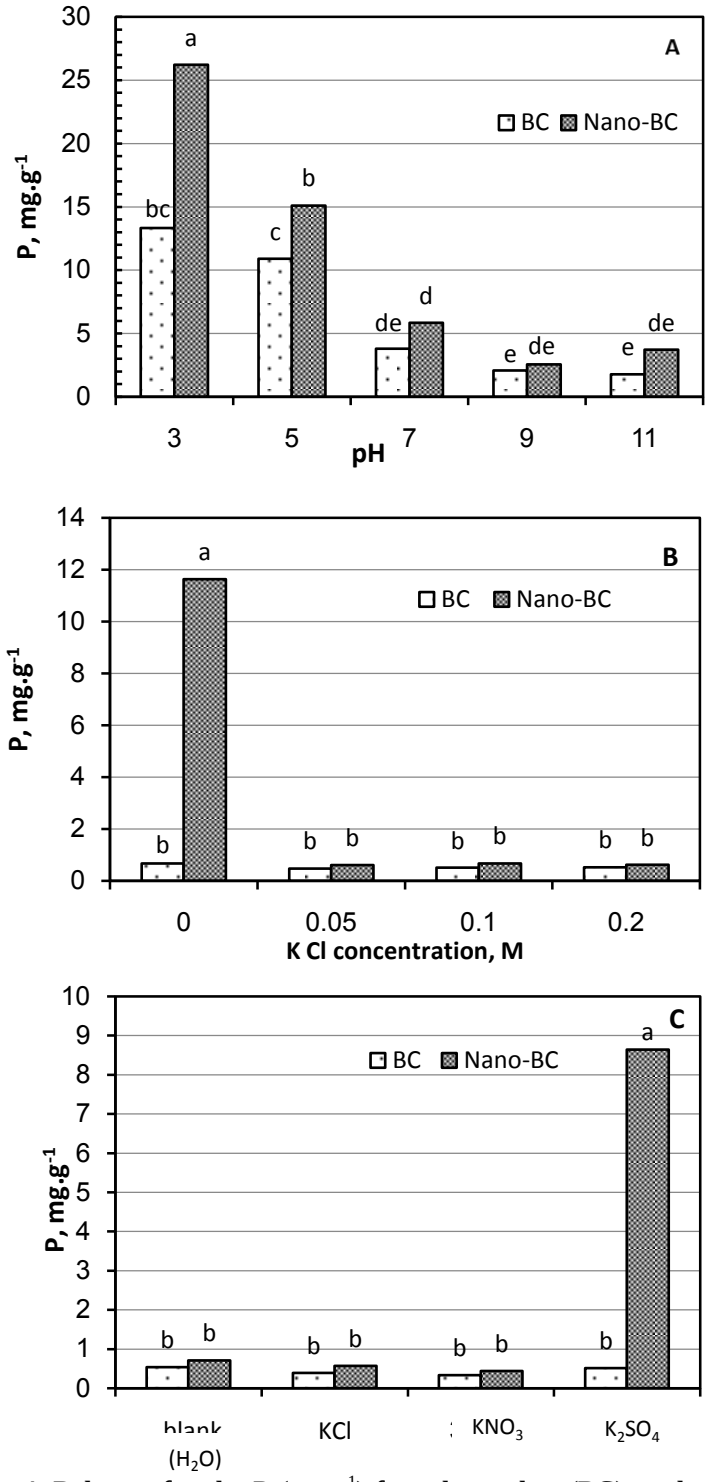

Fig. 4. Release of ortho-P (mg.g^{-1}**) from bone char (BC), and nano-bone char (Nano-BC) under different pH (A), different ionic strength (0.05, 0.1 and 0.2 M KCl concentrations)(B), and coexisting different anion (C)**
(Each column labeled by different letter (s) is statistically different at 0.05% level)

It is shown from Table (3) that the pseudo-second-order kinetic model was correlated well to the release ortho-P for all examined material. The regression coefficients (R^2) values were 0.894, and 0.901 for BC and Nano-BC(Fig.6 and Table.3). The agreement of the data with pseudo- second- order equation indicated the chemical nature of the release of ortho- P process, whereas the treatment temperature, during the pyrolysis process, of BC could change the mechanism towards diffusion (Qian et al. 2013; Xu et al., 2016; Huang et al., 2018). The pseudo-second-order constant rates (K_2) for Nano-BC (0.0007 d^{-1}) were higher than BC (0.0005 d^{-1}), suggesting the P formation in BC and Nano-BC is in stabilized formation. This could be attributed to type of P-speciation (non-orthophosphate) during the pyrolysis of bone (Huang and Tang 2015; Huang et al., 2018).

Conclusions

The performance of fast and slow P-releasing of Nano-BC was investigated compared to the originated BC. For fast P- release experiments, acidic pH was more suitable for the P-release from Nano-BC, while higher ionic strength conditions were not preferredand gave the lowest P-releasing amounts for BC and Nano-BC. Otherwise, the SO_4^{2-}coexisting anion enhanced the fast release of P form Nano-BC than those for Cl^- and NO_3^- . For the slow release tests, the pseudo-second-order kinetic model was governed model which indicated the chemical nature of the release of the ortho-P process from BC and Nano-BC. The results could support the potential of using Nano-BC as a P soil fertilizer.

TABLE 3 The obtained kinetic parameters of released ortho-P from bone char (BC), and nano-bone char (Nano-BC)

Model	BC	Nano-BC
Fractional power		
a	205.99	694.59
b	0.446	0.0154
R^2	0.806	0.007
Elovich		
α	538.36	5.44×10^{33}
β	0.0056	0.1065
R^2	0.740	0.004
Pseudo-first-order		
q_e	648.11	2136.26
k_1	-0.1257	-0.0015
R^2	0.416	0.039
Pseudo-second-order		
q_e	990.10	840.34
K_2	0.0005	0.0007
R^2	0.894	0.901
Intra-particle diffusion		
k_i	13.20	6.13
C	431.51	655.71
R^2	0.348	0.161

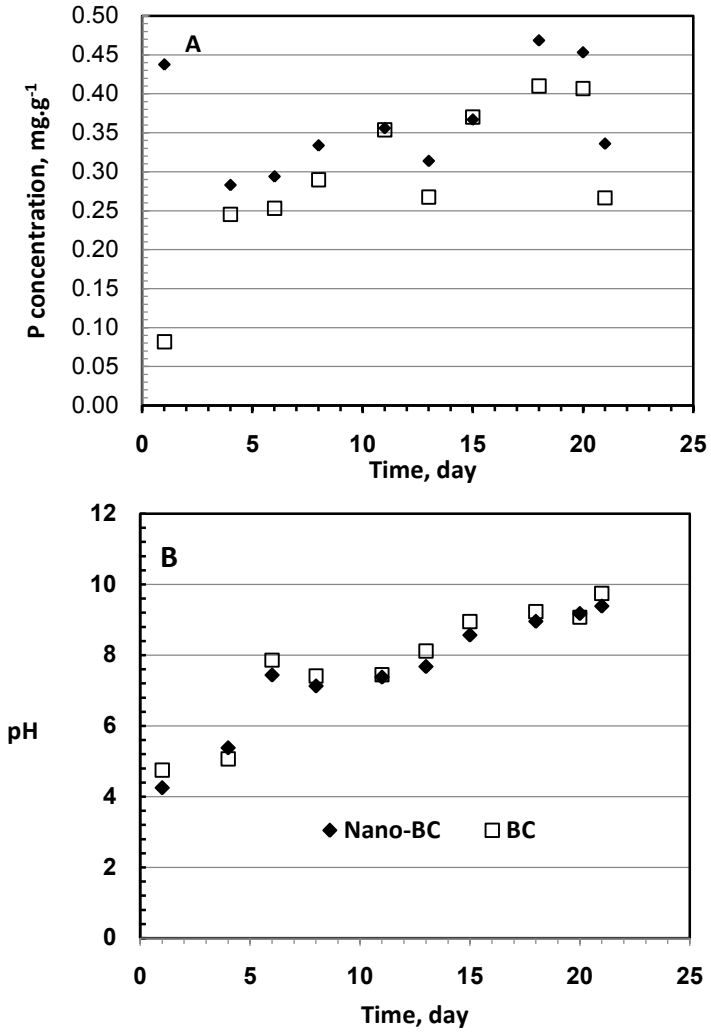

Fig. 5. P-released (orthophosphate) (A) from bone char (BC), and nano-bone char (Nano-BC) and changes in the solution pH (B) during the 21-day release cycle

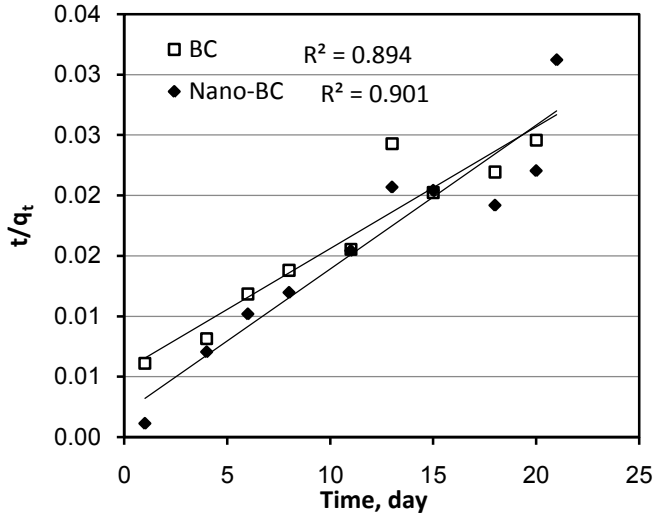

Fig. 6. Pseudo-second-order plots for ortho-P release kinetics from bone char (BC), and nano-bone char (Nano-BC)

References

Azzaouia K, Mejdoubi E, Lamhamdi A, Jodeh S, Hamed O, Berrabah M, Jerdioui S, Salghi R, Akartasse N, Errichd A, Ríos Á, Zougagh M (2017). Preparation and characterization of biodegradable nanocomposites derived from carboxymethyl cellulose and hydroxyapatite. *Carbohydrate Polymers*, **167**, 59–69. http://dx.doi.org/10.1016/j.carbpol.2017.02.092

Azzoui K, Mejdoubi E, Lamhamdi A, Zaoui S, Berrabah M, Elidrissi A, Hammouti B, Fouda M, Al-Deyab S (2015). Structure and properties of hydroxyapatite /hydroxyethyl cellulose. *Carbohydrate Polymers*, **115**, 170-176. http://dx.doi.org/10.1016/j.carbpol.2014.08.089

Black C A, Evans D D, White J L, Ensminger L E, Clark F E (1965). Methods of Soil Analysis.Parts 1 and 2.Am. Soc. Agron., Inc., Madison, Wisconsin, U.S.A.

Brunson L R, Sabatini DA (2014). Practical considerations, column studies and natural organic material competition for fluoride removal with bone char and aluminium amended materials in the Main Ethiopian Rift Valley. *Sci Total Environ.* 488–489, 580–587. https://doi.org/10.1016/j.scitotenv.2013.12.048

Buss W, Bogush A, Ignatyev K, Masek O (2020). Unlocking the fertilizer potential of waste-derived biochar. ACS Sustain *Chem Eng*, **8**, 12295–12303. https://doi.org/10.1021/acssuschemeng.0c04336

Buss W, Graham M C, Shepherd J G, Mašek O (2016). Suitability of marginal biomass-derived biochars for soil amendment. *Sci Total Environ*., **547**, 314–322. https://doi.org/10.1016/j.scitotenv.2015.11.148

Cazalbou S, Combes C, Eichert D, Rey C (2004). Adaptative physico-chemistry of bio-related calcium phosphates. *J. Mater. Chem.* **14**, 2148–2153. https://doi.org/10.1039/B401318B

Chapmann H D, Pratt P F (1961). Methods of Analysis for Soils, Plants and Waters. Div. Agric. Sci., Univ. of California, Berkeley.

Chen X, Yang L, Myneni SCB, Deng Y (2019) Leaching of polycyclic aromatic hydrocarbons (PAHs) from sewage sludge-derived biochar. *Chem Eng J.*, **373**, 840–845. https://doi.org/10.1016/j.cej.2019.05.059

Chen Z, Xiao X, Chen B, Zhu L (2015). Quantification of chemical states, dissociation constants and contents of oxygen-containing groups on the surface of biochars produced at different temperatures. *Environ Sci Technol.*, **49**, 309–317. https://doi.org/10.1021/es5043468

Chouyyok, W., Wiacek, R.J., Pattamakomsan, K., Sangvanich, T., Grudzien, R.M., Fryxell, G.E., Yantasee, W., 2010. Phosphate removal by anion binding on functionalized nanoporous sorbents. *Environ. Sci. Technol.*, **44**, 3073–3078. https://doi: 10.1021/es100787m

Cordell D, Rosemarin A, Schröder J J, Smit A L (2011). Towards global phosphorus security: A systems framework for phosphorus recovery and reuse options. *Chemosphere* **84**, 747–758. https://doi:10.1016/j.chemosphere.2011.02.032

Cordell D, Drangert J, White S (2009). The story of phosphorus: Global food security and food for thought. *Global Environmental Change*, **19**, 292-305. https://doi.org/10.1016/j.gloenvcha.2008.10.009

DeRosa M, MonrealC, Schnitzer M, Walsh R, Sultan Y (2010) Nanotechnology in fertilizers. *Nature Nanotechnology* , **5**,91. https://doi.org/10.1038/nnano.2010.2

Deydier E, Guilet R, Sarda S, Sharrock P (2005). Physical and chemical characterisation of crude meat and bone meal combustion residue: waste or raw material. *J. Hazard. Mater*. **121**, 141–148. https://doi.org/ 10.1016/j.jhazmat.2005.02.003

Elliott J C (2002). Calcium phosphate biominerals. In: Kohn M J, Rakovan J, Hughes J M (Eds.), Phosphates: Geochemical, Geobiological, and Materials Importance Reviews in Mineralogy and Geochemistry. Mineralogical Society of America, Chantilly, Virginia, pp. 427–453.

El-Ramady H ,Elbasiouny H , Elbehiry F , Zia-urRehman M (2021) Nano-Nutrients for carbon sequestration: A short communication. *Egyptian Journal of Soil Science*, **61**, 389 – 398. https://doi.org/10.21608/ejss.2021.107134.1480

El-Refaey A A, Mahmoud A H, Saleh M E (2015). Bone biochar as renewable and efficient P fertilizer: a comparative Study. *Alexandria J. Agric. Res.* **60**, 127-137.

El-Refaey A A (2021) Effect of Calcination and Ca-modified on Bentonite and Zeolite, with Respect to Phosphorus Removal from Aqueous Solution *Egyptian Journal of Soil Science*, **61**, 433 - 444. https://doi.org/10.21608/ejss.2022.108515.1482

Flores-Cano JV, Leyva-Ramos R, Carrasco-Marin F, Aragon-Piña A, Salazar-Rabago JJ, Levya-

Ramos S (2016) Adsorption mechanism of chromium (III) from water solution on bone char: effect of operating conditions. *Adsorption* **22**(3), 297–308. https://doi.org/10.1007/s10450-016-9771-3

França R, Samani T D, Bayade G, L'HocineYahia, Sacher E (2014) Nanoscale surface characterization of biphasic calcium phosphate, with comparisons to calcium hydroxyapatite and b-tricalcium phosphate bioceramics, *J. Colloid Interface Sci.,* **420**, 182–188. https://doi.org/10.1016/j.jcis.2013.12.055

Gilbert N (2009) The Disappearing Nutrient. Nature, 461 (7265), 716-8. https://doi.org/10.1038/461716a

Hashemi S, Rezaee A, Nikodel M (2013). Equilibrium and kinetic studies on the adsorption of sodium dodecylsulfate from aqueous solution using bone char. *ReacKinet Mech Cat.,* **109**:433–446. https://doi.org/ 10.1007/s11144-013-0559-0

Hernández-Hernández L E, Bonilla-Petriciolet A, Mendoza-Castillo D I, Reynel-Ávila H E (2017) Antagonistic binary adsorption of heavy metals using stratified bone char columns, *Journal of Molecular Liquids*, **241**, 334–346. https://doi: 10.1016/ j.molliq.2017.05.148

Huang R, Fang C, Zhang B, Tang Y (2018). Transformations of phosphorus speciation during (hydro) thermal treatments of animal manures. *Environ Sci Technol.,* **52**, 3016–3026. https://doi: 10.1021/acs.est.7b05203

Huang R, Tang Y (2015). Speciation dynamics of phosphorus during (hydro) thermal treatments of sewage sludge. *Environ Sci Technol.*, **49**,14466–14474. https://doi.org/10.1021/acs.est.5b04140

Ibrahim G A Z, Hegab R H (2022) Improving yield of barley using Bio and Nano Fertilizers under saline conditions. *Egyptian Journal of Soil Science,* **62**, 41 - 53. https://doi.org/10.21608/EJSS.2022.124377.1496

Kalia A, Kaur H (2019) Nano-biofertilizers: Harnessing Dual Benefits of Nano-nutrient and Bio-fertilizers for Enhanced Nutrient Use Efficiency and Sustainable Productivity. In: R. N. Pudake et al. (Eds.), *Nanoscience for Sustainable Agriculture*, https://doi.org/10.1007/978-3-319-97852-9_3, pp: 51 – 73. Springer Nature Switzerland AG

Kleemann R, Chenoweth J, Clift R, Morse S, Pearce P, Saroj D (2017). Comparison of phosphorus recovery from incinerated sewagesludge ash (ISSA) and pyrolysed sewage sludge char (PSSC).*Waste Manag* **60**:201–210. https://doi.org/10.1016/j.wasman.2016.10.055

Ko, D C K, Cheung CW, Choy K K H, Porter J F, McKay G (2004). Sorption equilibria of metal ions on bone char. *Chemosphere*, **54**, 273–281. doi:10.1016/j.chemosphere.2003.08.004

Koppelaar R H EM, Weikard H P (2013) Assessing phosphate rock depletion and phosphorus recycling options. *Global Environmental Change*, **23**, 1454–1466. http://dx.doi.org/10.1016/j.gloenvcha.2013.09.002.

Lanyon L E, Heald W R (1982) Magnesium, calcium, strontium and barium. In: Page A L, Miller R H, Keeny D R (Eds.). Methods of Soil Analysis, Part 2. Chemical and Microbiological Properties.Agronomy Monograph No. 9 (2nd Edition).ASA-ASSA, Madison, USA.

Leyva-Ramos,R., J. Rivera-Utrilla, N.A. Medellin-Castillo, M. Sanchez-Polo, (2010) Kinetic modeling of fluoride adsorption from aqueous solution onto bone char, *Chem. Eng. J.* **158**, 458–467. https://doi.org/10.1016/j.cej.2010.01.019

Liu Q, Li J, Fang Z, Liu Y, Xu Y, Ruan X, Zhang X, Cao W (2021) Behavior of fast and slow phosphorus release from sewage sludge–derived biochar amended with CaO. *Environmental Science and Pollution Research*, **28**, 28319–28328. https://doi.org/10.1007/s11356-021-12725-z

Maeda C H, Araki C A, Moretti A L, Maria de Barros A S D, Arroyo P A (2019). Adsorption and desorption cycles of reactive blue BF-5G dye in a bone char fixed-bed column. *Environmental Science and Pollution Research* (2019) **26**:28500–28509. https://doi.org/10.1007/s11356-018-3644-0

Mahaletchumi S (2021) Review on the Use of Nanotechnology in Fertilizers. *Journal of Research Technology and Engineering*, **2**, 60-72.

Mahmoud A H, Saleh M E, El-Refaey A A (2017). Evaluation of poultry manure and acidified water for improving phosphorus utilization from bone char: a comparative study. *Egyptian Journal of Soil Science,* **57**, 233 – 245. https://doi.org/10.21608/EJSS.2017.928.1101

Mahmoud E, El Baroudy A, Ali N, Sleem M (2020). Spectroscopic studies on the phosphorus adsorption in salt-affected soils with or without nano-biochar additions. *Environmental Research*, **184**, 109277. https://doi.org/10.1016/j.envres.2020.109277

Manalu J L, Soegijono B, Indrani D J (2015). Characterization of Hydroxyapatite Derived from Bovine Bone, *Asian Journal of Applied Sciences*, **3** (4), 758- 765.

Mastronardi E, Tsae P, Zhang X, Monreal C, DeRosa M C (2015). Strategic Role of Nanotechnology in Fertilizers: Potential and Limitations. In: Rai M, Ribeiro C, Mattoso L, Duran N (Eds) Nanotechnologies in Food and Agriculture. Springer, Cham. https://doi.org/10.1007/978-3-319-14024-7_2

Medellin-Castillo, N.A., Leyva-Ramos, R., Padilla-Ortega, E., Perez, R.O., Flores-Cano, J.V., Berber-Mendoza, M.S., 2014. Adsorption capacity of bone char for removing fluoride from water solution. Role of hydroxyapatite content, adsorption mechanism and competing anions. *J. Ind. Eng. Chem.* **20**, 4014–4021. https://doi.org/10.1016/j.jiec.2013.12.105.

Mesquita P, Souza C R, Santos N T G, Rocha S D F (2018) Fixed-bed study for bone char adsorptive removal of refractory organics from electrodialysis concentrate produced by petroleum refinery. *Environ. Technol.*, **39**, 1544–1556. https://doi.org/10.1080/09593330.2017.1332691

Nader M (2015). Surface area: Brunauer–Emmett–Teller (BET). In: Progress in Filtration and Separation (S. Tarleton, ed.). Academic Press, London, UK, pp. 585–608.

Nazeer M A, Yilgör E, Yilgör I (2017) Intercalated chitosan/hydroxyapatite nanocomposites: Promising materials for bone tissue engineering applications. *Carbohydrate Polymers* **175**, 38–46. http://dx.doi.org/10.1016/j.carbpol.2017.07.054

Olsen S R, Sommers L E (1982) Phosphorus. In Page A L et al. (ed.) Chemical and microbiological properties. 2nd ed. ASA, Madison, WI. , pp. 403-427.

Pasteris, J D, Yoder C H, Sternlieb M P, Liu S (2012) Effect of carbonate incorporation on the hydroxyl content of hydroxylapatite. *Mineral. Mag.* **76**, 2741–2759. https://doi.org/10.1180/minmag.2012.076.7.08

Patel S, Han J, Qiu W, Gao W (2015). Synthesis and characterisation of mesoporous bone char obtained by pyrolysis of animal bones, for environmental application. *J. Environ. Chem. Eng.* **3**, 2368-2377. doi:10.1016/j.jece.2015.07.031.

Qian T, Zhang X, Hu J, Jiang H (2013) Effects of environmental conditions on the release of phosphorus from biochar. *Chemosphere*, **93**, 2069–2075. https://doi.org/10.1016/j.chemosphere.2013.07.041

Rittmann B E, Mayer B, Westerhoff P, Edwards M (2011) Capturing the lost phosphorus. *Chemosphere*, **84**, 846–853. https://doi.org/10.1016/j.chemosphere.2011.02.001

Rocha S D F, Ribeiro M V, Viana P R M (2011) Bone char: an alternative for removal of diverse organic and inorganic compounds from industrial wastewater. In: AmitBhatnagar (Org.). Application of Adsorbents for Water Pollution: Bentham Science; 2011, v. 14. Available from: http://www.benthamscience.com/ebooks/forthcomingtitles.htm

Rojas-Mayorga C K, Bonilla-Petriciolet A., Aguayo-Villarreal I A, Hernández-Montoya V, Moreno-Virgen M R, Tovar-Gómez R, Montes-Morá M A, (2013). Optimization of pyrolysis conditions and adsorption properties of bone char for fluorideremoval from water. *Journal of Analytical and Applied Pyrolysis*, **104**, 10-18. https://doi.org /10.1016/j.jcis.2013.12.055

Saleh E M, El-Refaey AA, El-Damarawy Y A (2020). CO2 emissions and soil organic carbon in calcareous soils as affected by bone char and phosphate rock. *Egyptian Journal of Soil Science*, **60**, 365-375. https://doi.org/10.21608/ejss.2020.32612.1363

Saleh M E, El-Refaey A A, MahmoudA H. (2016). Effectiveness of sunflower seed husk biochar for removing copper ions from wastewater: a comparative study. *Soil & Water Res.*, **11**(1), 53–63. https://doi.org/10.17221/274/2014-SWR

Siebers N F, Leinweber P (2013). Bone char: a clean and renewable phosphorus fertilizer with cadmium immobilization capability. *Journal of Environmental Quality.* **42**, 405–411. https://doi.org/10.2134/jeq2012.0363

Smil V (2000) Phosphorus in the environment: natural flows and human interferences. *Annu. Rev. Energy Environ.* **25**, 53-88. https://doi.org/10.1146/annurev.energy.25.1.53

Warren G P, Robinson J S, Someus E (2009). Dissolution of phosphorus from animal bone char in 12 soils. *Nutr.t Cyc. Agroecosyst*, **84**,167–178. https://doi.org/10.1007/s10705-008-9235-6

Weber B, Stadlbauer E A, Schlich E, Eichenauer S, Kern J, Steffens D (2014) Phosphorus bioavailability of biochars produced by thermo-chemical conversion. *J. Plant. Nutr. Soil Sci.*,

177, 84–90. https://doi.org/10.1002/jpln.201300281

Wilson J A, Pulford I D, Thomas S (2003) Sorption of Cu and Zn by bone charcoal. *Environmental Geochemistry and Health* **25**: 51–56, 2003. https://doi.org/10.1023/a:1021288529358

Xu G, Zhang Y, Shao H, Sun J (2016). Pyrolysis temperature affects phosphorus transformation in biochar: Chemical fractionation and 31P NMR analysis. *Sci. Total Environ*, 569–570, 65–72. https://doi.org/10.1016/j.scitotenv.2016.06.081

Younesi M, Javadpour S, Bahrololoom M E (2011). Effect of heat treatment temperature on chemical compositions of extracted hydroxyapatite from bovine bone ash. *Journal of Materials Engineering and Performance*, **20**: 1484–1490. https://doi.org/10.1007/s11665-010-9785-z

Zwetsloot M J, Lehmann J, Bauerle T, Vanek S, Hestrin R, Nigussie A (2016). Phosphorus availability from bone char in a P-fixing soil influenced by root-mycorrhizae-biochar interactions. *Plant Soil.* **408**, 95-105. https://doi.org/10.1007/s11104-016-2905-2

Zwetsloot M J, Lehmann J, Solomon D (2014). Recycling slaughterhouse waste into fertilizer: how do pyrolysis temperature and biomass additions affect phosphorus availability and chemistry? *Journal of the Science of Food and Agriculture.* **95**, 281–288. https://doi.org/10.1002/jsfa.6716